Ureña, J., Tsipas, S., Jiménez-Morales, A., Gordo, E., Detsch, R., Boccaccinic, A.R. (2018). In-vitro study of the bioactivity and cytotoxicity response of Ti surfaces modified by Nb and Mo diffusion treatments. *Surface and Coatings Technology*, 335, pp. 148-158.

DOI: https://doi.org/10.1016/j.surfcoat.2017.12.009

In-vitro study of the bioactivity and cytotoxicity response of Ti surfaces modified by Nb and Mo diffusion treatments

J. Ureña, S. Tsipas, A. Jiménez-Morales, E. Gordo, R. Detsch, A.R. Boccaccini

PII: S0257-8972(17)31226-4
DOI: doi:10.1016/j.surfcoat.2017.12.009
Reference: SCT 22927

To appear in: *Surface & Coatings Technology*

Received date: 28 August 2017
Revised date: 2 December 2017
Accepted date: 4 December 2017

Please cite this article as: J. Ureña, S. Tsipas, A. Jiménez-Morales, E. Gordo, R. Detsch, A.R. Boccaccini , In-vitro study of the bioactivity and cytotoxicity response of Ti surfaces modified by Nb and Mo diffusion treatments. The address for the corresponding author was captured as affiliation for all authors. Please check if appropriate. Sct(2017), doi:10.1016/j.surfcoat.2017.12.009

In-vitro study of the bioactivity and cytotoxicity response of Ti surfaces modified by Nb and Mo diffusion treatments

J. Ureña [1], S. Tsipas [1, 2], A. Jiménez-Morales [1, 2], E. Gordo [1, 2], R. Detsch [3], A. R. Boccaccini [3]

[1] *UNIVERSITY CARLOS III OF MADRID, Department of Materials Science and Engineering, IAAB, Avda. Universidad, 30, 28911 Leganés, Spain.*
jurena@pa.uc3m.es; stsipas@ing.uc3m.es; toni@ing.uc3m.es; elena.gordo@uc3m.es

[2] *ALVARO ALONSO BARBA TECHNOLOGICAL INSTITUTE OF CHEMISTRY AND MATERIALS, University Carlos III of Madrid*

[3] *INSTITUTE OF BIOMATERIALS, Department of Materials Science and Engineering, University of Erlangen-Nuremberg, 91058 Erlangen, Germany.*
rainer.detsch@ww.uni-erlangen.de; aldo.boccaccini@ww.uni-erlangen.de

Abstract

This work focuses on the bioactivity and biological response of modified Ti surfaces produced by powder metallurgy. They are processed by diffusion of two β-stabilizing elements, Nb and Mo, deposited onto the surface of PM Ti substrates. Moreover, the addition of an activating agent, NH_4Cl, to the suspension has been carried out by thermo-reactive diffusion process. The surface modification led to a gradient in composition (Ti-Nb or Ti-Mo) and microstructure (β – α+β – α phases). This work presents the bioactivity results of these Ti-Mo and Ti-Nb surfaces as well as the cell-material response of the Ti-Nb surfaces. The reactivity of the materials was tested through immersion in simulated body fluid considering Ca and P precipitation in order to assess the ability of the materials to induce hydroxyapatite formation. The in-vitro cell response was evaluated by human osteoblast-like cells incubation on the different surfaces for 48 hours. The investigation led to positive results in terms of surface bioactivity and an improved cell-material interaction of the PM modified Ti-Nb surfaces compared to the reference Ti material.

KEYWORDS: β-gradient Titanium, Surface modification, Powder technology, Bioactivity, Cytotoxicity.

1. Introduction

The current tendency toward designing and developing β-type Ti alloys comes from the complexity of the requirements needed for biomaterials. This new generation of Ti alloys perfectly combines the requirements for bone replacement applications [1]. These are mainly related to the lower Young's modulus compared to those of the first generation Ti alloys such as the commercially pure CP-Ti (α-type) and Ti6Al4V (α+β type). Although both of them are extensively used; their superior Young's modulus (≈ 110 GPa) compared to that of human bone (≈ 30 GPa) results in higher stiffness which is the main cause of bone resorption [2], [3], [4]. However unlike the first generation, β-Ti alloys offer better mechanical performance together with higher biocompatibility [5]. In this sense, this generation is characterized by the addition of non-toxic elements (Nb, Mo, Ta, Zr); discarding harmful elements (Ni, Al or V) in order to avoid dangerous effects [6]. This requirement is considered of extreme importance to eliminate or reduce toxic effects on cells through metal ion release. This effect can be inhibited by the presence of Nb or Mo since they stabilize the oxide layer formed (Nb_2O_5); contributing to better surface integrity and thus, avoiding possible subsequent adverse reactions [7]. Besides the toxic effect of the metallic ions, the biocompatibility is affected by the bioactivity and the cell-material interaction. An *in vitro* bioactivity analysis permits to predict the in vivo bio-reactivity response of an implant, giving an idea of its bone-bonding ability and its bioinert or bioactive character. Generally, the first generation of Ti alloys is considered as bioinert because of their lack of apatite formation on its surfaces. However, the bioinert or bioactive character can be altered through surface modification; enhancing the bioactivity and osseointegration [8], [9], [10]. Nonetheless, there is evidence that some β-type Ti alloys are included among bioactive biomaterials since the addition of some alloying elements (Nb, Mo, Sn) respond positively to the

apatite-forming ability [11]. Therefore, the success of an implant not only requires careful properties tailored from metallurgical processing but also excellent biocompatibility. The concept of biocompatibility has been redefined along time but in essence, the biocompatibility of an implant is associated to not create inflammatory adverse response at the same time that stimulating osseointegration [12].

In the case of metals, the poor bioactivity and toxic ions release in the human body are the main challenges to face in order to improve the performance of implants. Surface treatment techniques are employed to enhance biocompatibility through better interface between implant and surrounding living tissues. These surface treatments are based on modifying the chemistry and microstructure of the surface or applying coatings. First, among the surface treatments to modify the surface are found: i) sand-blasting to provide roughness values from 0.3 to 3 μm, ii) wet-etching to modify morphology and induce the apatite formation, iii) use of electron beams to deposit CaP layers, or iv) introducing some specifically biocompatible elements (Nb, Mo, Sn or Sr) [13]. Secondly, bioactive coatings can be applied by: i) physical vapor deposition (PVD), ii) plasma spray, iii) laser cladding or iv) sol-gel and electrochemical deposition [14].

In recent works, the presence of Nb as alloying element in titanium or dopant agent in bioceramics has created potential interest due to the excellent biocompatibility and lack of reactivity in body fluid environment [15], [16], [17]. Similar to Nb, Mo is also considered as another β-stabilizer element with good cytocompatibility and no cytotoxic effect [9] as well as stronger β-character and thus, as stronger ability of β-phase formation compared to Ta or Zr [6]. Therefore, the bioactivity of some of these β-Ti alloys needs to be investigated in order to understand better their apatite formation ability on their surfaces after immersion in simulated body fluid (SBF) [18]. In most of the investigations, the bioactivity of the alloys is studied after different surface

treatments (mechanical, chemical or electrochemical methods) in order to promote the apatite nucleation on their surfaces [10]. This is the case of a recent research where the bioactivity of the Ti-27Nb-13Zr prepared by powder metallurgy and chemically treated in NaOH before the immersion in SBF was investigated [19]. Nevertheless, an additional surface treatment is not always useful if the aim is to test a specific composition with designed properties. Hence, similar compositions (Ti-7.5Mo-2Fe and Ti-15Mo-2.8Nb) have been immersed in SBF for long periods of time without extra surface treatments, showing good results in terms of bioactive precipitate formation [20]. Additionally, the attractiveness of these elements is increasing due to their good *in vitro* response on cell adhesion, proliferation and also osteogenic differentiation [21], [22].

In a previous study we reported on the gradient in microstructure (β – α+β – α) of these surfaces together with their mechanical performance. An improvement in hardness and decreased elastic modulus were successfully achieved through diffusion treatments [22]. Furthermore, the chemical modifications performed by Nb and Mo should not deteriorate the requirement of biocompatibility, but on the contrary they are expected to improve it. Therefore, in this study we explored the bioactivity and cell-material response of different Ti-Nb and Ti-Mo materials prepared by powder metallurgy plus surface modification through diffusion processes. On one side, the bioactivity of Ti-Mo and Ti-Nb surfaces was directly tested by immersion in simulated body fluid (SBF) without any additional pre-treatment of the materials to stimulate the hydroxyapatite formation. On the other side, human osteoblast-like cells (MG-63) were cultured on different Ti-Nb surfaces to compare cell viability and proliferation, cell adhesion, distribution and morphology features.

2. Experimental procedure

2.1 Modified Ti material preparation

To obtain the different modified PM Ti surfaces, the Ti material used as starting point was processed by powder metallurgy in a conventional route of pressing and sintering. For the fabrication of the titanium substrates, Ti hydride powder (GfE Metalle und Materialien GmbH, Germany) with particle size below 63 μm was used. This Ti powder allowed minimization of the oxidation effect and the cost of production by means of lower sintering temperature and shorter sintering time; obtaining higher final relative density values [24]. First, green compacts were obtained after uniaxial pressing at room temperature and 600 MPa by using a cylindrical mold of 16 mm in diameter with walls lubricated by zinc stearate. Then, they were sintered in high vacuum (10^{-5} mbar) at 1100 ^{o}C for 1 h with a heating and cooling rate of 5 ^{o}C/min. This pressing and sintering processes led to the reference Ti material. Ti surface was finished after a polishing step with alumina up to 1 μm. On the other hand, the modified PM Ti surfaces were designed after obtaining the sintered Ti substrates, according to different parameters: 1) diffusion of elements (Nb or Mo), 2) treatment process (diffusion or thermo-reactive diffusion), and 3) final surface condition (polished, ground or as-coated). In Table 1 the routes followed for the processing of the materials and their nomenclature used further on are summarized.

Initially, the Nb or Mo was deposited through spraying an aqueous suspension of Nb or Mo onto the sintered Ti substrates after grinding with 180# SiC emery paper in order to remove any possible oxides formed. The details of the processing procedure of the suspensions are given elsewhere [23]. The deposited elements (Nb or Mo) were diffused into the substrate by a heat treatment in high vacuum (10^{-5} mbar) at 1100 ^{o}C during 3 h to guarantee the diffusion processes and the microstructural change with the β-phase

formation. These diffusion conditions were selected according to our previous works [25], [26]. Thus, the process led to the samples Ti-Nb_{coat} and Ti-Mo_{coat}. However in order to evaluate both the compositional changes and the effect of surface roughness, a soft grinding step with a 1200# SiC emery paper was performed to obtain the same materials but with a different final surface state [23]. The grinded materials were labelled as Ti-Nb and Ti-Mo. On the other hand, The Ti-Nb_{NH4Cl} and Ti-Mo_{NH4Cl} materials were processed through thermo-reactive process in a controlled Ar atmosphere. Finally, all of them were finished in propanol ultrasonic bath cleaning for 10 min followed by distilled water washing during 5 min.

Table 1. Different designing parameters of the materials prepared.

Design materials	***Design parameters***						
	Diffusion Element		**Diffusion Process**		**Final surface state**		
	Nb	*Mo*	*Diffusion*[(1)]	*TRD*[(2)]	*Polished (1µm)*	*Ground (1200#)*	*As-coated (Untreated)*
Ti	-	-	-	-	*x*		
Ti-Nb	*x*		*x*			*x*	
Ti-Nb_{coat}	*x*		*x*				*x*
Ti-Nb_{NH4Cl}	*x*			*x*		*x*	
Ti-Mo		*x*	*x*			*x*	
Ti-Mo_{coat}		*x*	*x*				*x*
Ti-Mo_{NH4Cl}		*x*		*x*		*x*	

(1) In high vacuum
(2) Thermo-reactive diffusion (in Ar atmosphere with activator agent (NH_4Cl))

2.2 Surface characterization

Surface examinations were carried out by field emission-scanning electron microscopy (FE-SEM FEI, Teneo) and the surface chemical constitution was determined with EDAX, energy dispersive X-ray spectroscopy (EDS). The chemical composition of each sample was obtained by analyzing five areas of 20 µm x 40 µm. The final surface roughness was determined by Hommel tester T500 profilometer and the average roughness parameter, R_a, was obtained. All samples were measured in triplicate. Wettability of the samples was evaluated by measuring the contact angle (DSA 30

Kruss, Germany). A 3 µl water drop was delivered to the final surfaces at room temperature. Contact angle was determined on three samples for each material and three measurements per sample to provide an average and standard deviation of the results.

2.3 Bioactivity analysis

The reactivity of the different materials was tested through simulated body fluid (SBF) immersion assays attending to the Ca and P precipitation in order to see the ability of hydroxyapatite formation. A SBF solution was prepared according to Kokubo's method [18] and two specimens of each designed material were immersed for a period of two and three weeks at 37^{o}C and pH of 7.4. The hydroxyapatite formation by precipitation of Ca and P ions and surface morphology changes were examined by Fourier transform infrared spectroscopy (FTIR), x-ray diffraction (XRD) and field emission scanning electron microscopy (FE-SEM).

Fourier transformed infrared (FTIR) spectra (Impact 420, Nicolet Instr., US) were recorded in the frequency range 400-4000 cm^{-1}. The spectra were measured using an ATR accessory with torque-limited pressure device (DuraSampIIR^{TM} II, Smiths Detection) for sampling. Samples were analyzed after 14 and 21 days immersion in SBF.

X-ray diffraction measurements in grazing incidence condition (GIXRD) were carried out with a Bruker AXS D8 diffractometer equipped with an X-ray Co tube operating at 40kV and 30 mA and Goebel mirror optics to obtain a parallel and monochromatic X-ray beam. 2θ scans over a range from 25 to 100º were performed at an angle of incidence of 5° with a step width of 0.02º and a counting time of 3 s/step. The phase present in the XRD patterns were identified by the search-match technique using the DIFFRACplus EVA software by Bruker AXS and the JCPDS data base. The 4.2 version of Rietveld analysis program TOPAS (Bruker AXS) was used to model the full pattern

with the phases identified after a first search/match routine and to reveal the presence of additional minor phases in the difference pattern.

Hydroxyapatite morphology was analyzed by FE-SEM (2 kV acceleration and 6-8 mm working distance) after 14 and 21 days of immersion in SBF.

2.4 Cell culture

For the cell culture study, the selected samples were those with Nb as the diffusion element due to the great interest presented in this biocompatible element as well as their deeper (β-α+β) diffusion areas.

Human osteoblasts-like cells (MG-63) were cultured in Dulbecco's modified eagle's culture medium (DMEM) containing 10 % fetal calf serum (FCS) and 1 % antibiotics (penicillin + glutamine) at 37 ^{o}C in humidified atmosphere of 5% CO_2 in air. The medium was changed with an interval of 2-3 days to prevent cell death; it was washed with 6 mL of phosphate-buffered saline solution (PBS) and incubated with ≈ 1 mL of trypsin/EDTA in order to evaluate cell detachment. Thereafter, 9 mL of DMEM was added for the inhabitation of the trypsin effect. Previously, samples were sterilized by steam autoclaving at 121 ^{o}C for 90 minutes and they were dried overnight. Later, they were placed in untreated well plates of ≈ 1.9 cm^2 surface area per well. Cells were counted and seeded onto the well-plates containing all the different samples: Ti, Ti-Nb, $Ti\text{-}Nb_{coat}$ and $Ti\text{-}Nb_{NH4Cl}$. The density of the cells cultured was of 3.3 x 10^5 cells/mL per well and they were incubated for 48 hours. Five samples of each material were used for cell viability, three for adhesion, distribution and morphology; and two for SEM inspection.

2.4.1 Cell viability test

Cellular viability of MG-63 cells on the three modified Ti surfaces plus a Ti control was assessed after 48 hours using a commercial Cell Counting Kit-8 (CCK-8) via WST-8 [2-(2-methoxy-4-nitrophenyl)-3-(4-nitrophenyl)-5-(2,4- disulfophenyl)-2H-tetrazolium, monosodium salt over 48 hours of incubation. CCK-8 allows sensitive colorimetric assays in order to determine the number of viable cells in cell proliferation and cytotoxicity assays. WST-8 acts as a colorimetric indicator which is reduced by dehydrogenases in cells to give a yellow colored product (formazan), which is soluble in the tissue culture medium. The amount of the formazan dye generated by the activity of dehydrogenase in cells is directly proportional to the number of living cells. This test gets higher sensitivity detection than other tetrazolium salts used as MTT, XTT or MTS. For this test, a mixture preparation of 1 % WST + 99 % DMEM was prepared and an amount of 0.75 mL was added in each sample. After 2 hours, the reaction was completed and prepared for the measurement.

2.4.2 Calcein staining

After 2 days of incubation, the samples were also evaluated for cell adhesion, distribution and morphology using laser confocal fluorescent microscope (DM6000 CFS, Leica, Germany). For this purpose, Calcein was the cell-permeable dye chosen due to its ability for determining cell viability in most eukaryotic cells. The medium of the well plates containing the samples and the blanks was removed; and a 4 μL/mL calcein solution was prepared. A volume of 45 μL Calcein was put in 11.21 mL of PBS and 0.75 mL of the mixture was added in each sample. Finally, the samples need to be removed from the well plates, covered with PBS and stored in the dark. Three images at 20x magnification of each sample (in total 6 images of each material) were acquired and the number of cell was counted by ImageJ software.

2.4.3 Examination by SEM

SEM analysis of the samples was carried out after 2 days of culture by FE-SEM. For the preparation, they were rinsed with PBS buffer to remove the culture medium and after, two fixing solutions were added with a waiting time of 1 hour each. Before the SEM observation, all the samples were dehydrated by immersion in a set of ethanol solutions of increasing concentration. The finishing process was carried out applying an extra thin gold coating by mean of a sputter coater device.

2.4.4 Statistical analysis

Cell viability experiment was repeated with five samples and the number of cell adhered with three samples. Cell viability and number of cell adhered results are presented as an average and standard deviation of ten and six measurements of each material, respectively. Unmodified Ti samples (Ti) were set as 100 %. The results were evaluated by one-way analysis of variance (ANOVA, Tukey test) to determine statistical significant differences between the means of the different groups. The level of the statistical significance is given by *p*-values ($p < 0.05$ *no significant,* $p > 0.05$ *significant*) calculated by Origin software (version 8.5, OriginPro).

3. Results and discussion

3.1 Chemical composition and microstructural surface characterization

Results of EDS analysis showing the chemical constitution in weight percentage of all the modified Ti surfaces can be observed in Table 2. The EDS analysis was performed on treated surfaces (Ti-Nb and Ti-Mo) after removing some possible oxide formed, and on untreated surfaces (Ti-Nb_{coat}, Ti-Nb_{coat}, Ti-Nb_{NH4Cl} and Ti-Mo_{NH4Cl}). It was carried out by means of analyzing five different areas of 20 μm x 40 μm. These measurements were performed after preparing the surfaces according to the final surface states

summarized in Table 1. This summarizes the variety of the designed surfaces in terms of composition (%): *a) Niobium as* diffusion element: Ti-Nb {65, 35}; Ti-Nb_{coat} {1, 99}; Ti-Nb_{NH4Cl} {82, 1, 8 (O), 9 (N)}, *b) molybdenum as diffusion element*: Ti-Mo {82, 18}; Ti-Mo_{coat} {1, 99}; Ti-Mo_{NH4Cl} {86, 1, 7 (O), 6 (N)}.

Table 2. EDS analysis of the modified PM Ti surfaces showing the chemical composition for: Ti-Nb, Ti-Nb_{coat}, Ti-Nb_{NH4Cl}, Ti-Mo, Ti-Mo_{coat}, Ti-Mo_{NH4Cl}.

Material	Ti [%]	Nb [%]	Mo [%]	O [%]	N [%]
Ti-Nb	65	35	-	-	-
Ti-Nb_{coat}	1	99	-	-	-
Ti-Nb_{NH4Cl}	82	1	-	8	9
Ti-Mo	82	-	18	-	-
Ti-Mo_{coat}	1	-	99	-	-
Ti-Mo_{NH4Cl}	86	-	1	7	6

Figure 1 presents the scanning electron micrographs of the surfaces for the different materials. The surface modification with Nb or Mo led to similarities in terms of microstructure. However, differences are found due to the three different surface-finishing processes (polish, grinding or as-coated) selected. In the case of Ti-Nb/Ti-Mo, the extremely soft grinding and polishing step lead to a fine and homogeneous microstructure composed of very close and compact β lamellas; obtaining β-phase surfaces for both materials. On contrary, the coated samples (Ti-Nb_{coat}/Ti-Mo_{coat}) presented a surface of Nb or Mo powder micro-particles due to the lack of surface finishing treatment after obtaining the material with the aim of testing rougher surfaces completely composed of Nb or Mo. Finally, the thermo-reactive diffusion process led to Ti-Nb_{NH4Cl}/Ti-Mo_{NH4Cl} materials with porous microstructures and few and separated β lamellas. From the combination of EDS and microstructure studies, the surfaces were evaluated in terms of composition, roughness and porosity.

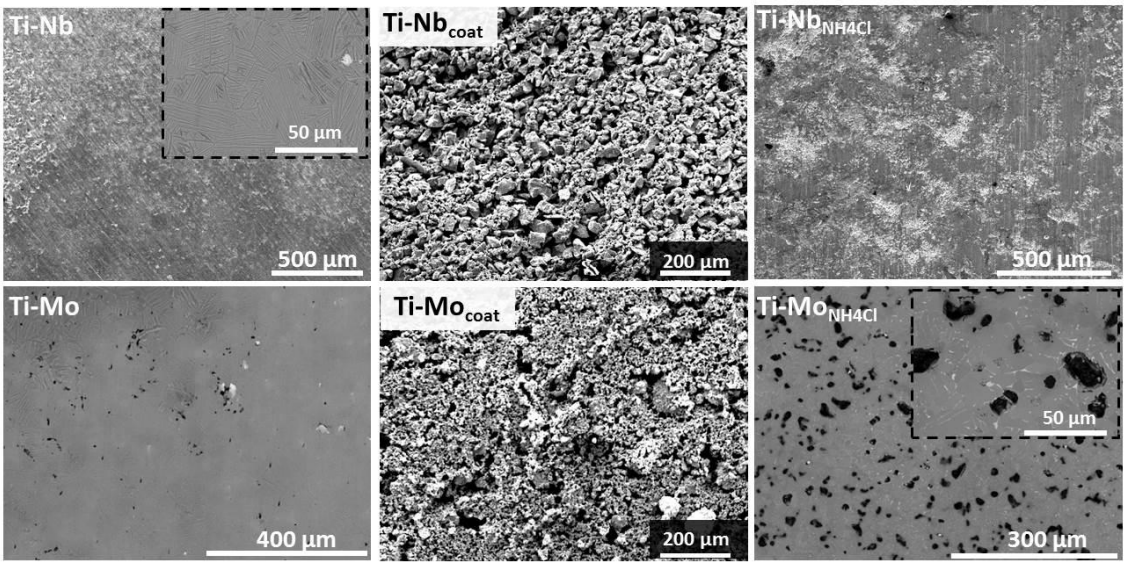

Figure 1. SE SEM micrographs of the surfaces for the designed modified PM Ti materials: Ti-Nb, Ti-Nb_{coat}, Ti-Nb_{NH4Cl}, Ti-Mo, Ti-Mo_{coat}, Ti-Mo_{NH4Cl}

The microstructure and composition analysis of these modified Ti surfaces together with the variation along depth and the mechanical performance has previously been presented elsewhere [23], [25]. They showed an improved hardness of 4-5 GPa (twice the hardness of cp-Ti). The value of elastic modulus was 64 GPa (Ti-Nb) and 63 GPa (Ti-Mo), compared to 110 GPa of cp-Ti [23]. As an example of the cross-section of the designed surfaces, Ti-Mo and Ti-Mo_{NH4Cl} surfaces are shown in Figure 2. Mo or Nb diffusion led to a similar microstructure composed of a gradient of phases β / α+β / α as observed in Figure 2a. On the other hand, the Mo or Nb thermo-reactive diffusion treatment created the nitride and porous Ti surface as shown in Figure 2b for the case of Ti-Mo_{NH4Cl}. The variation in composition along depth is presented in Figure 2c by means of EDS analysis taken from the marked areas. The Mo diffusion treatment created a Mo-rich region (46 % Mo) closer to surface and a bi-phasic α+β region due to the decrease in Mo content along depth leading the final α un-altered Ti structure. In the case of the Ti-Mo_{NH4Cl} surface, a TiN layer was created in surface and a porous layer with some Mo was confirmed due to the use of the NH_4Cl activator.

a) b)

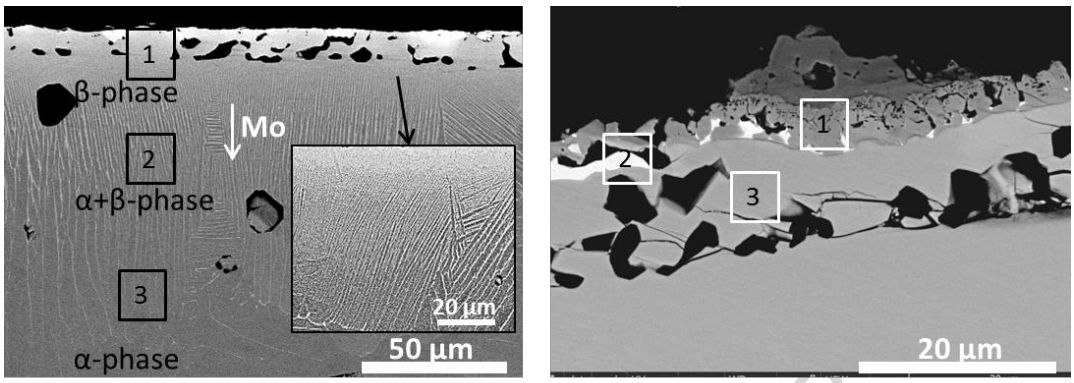

c)

Material	Marked areas	Ti [wt%]	Mo [wt%]	N [wt%]	O [wt%]
Ti-Mo	Z1	53.9	46.1	-	-
	Z2	89.8	10.2	-	-
	Z3	97.9	2.1	-	-
$Ti\text{-}Mo_{NH4Cl}$	Z1	83.4	2.5	8.6	5.5
	Z2	69.4	25.5	5.1	-
	Z3	89.5	-	10.5	-

Figure 2. Cross-sectional SE SEM images of: a) Ti-Mo and b) $Ti\text{-}Mo_{NH4Cl}$ surfaces. c) EDS values from selected areas.

3.2 Surface roughness and wettability characterization

The surface roughness and wettability results are shown in Figure 3. Both of these parameters are recognized by their significance on cell interaction with the biomaterials. However, other physical-chemical properties such as surface energy, texture, chemical composition, morphology or surface charge also have been shown to affect cell response [8], [27]. Most of these properties are related to each other and the change in one of these properties could lead to the modification of another, such as roughness which can modify the correlation between the surface energy and cell proliferation. It has been difficult to establish general rules because cell response is affected by the cell phenotype (osteoblast, fibroblast…) and the protein adsorption, among other factors. Nevertheless, the measurement of surface roughness and wettability has been considered as essential to determine the adhesion and the hydrophilic-hydrophobic behaviour of the material, respectively. Figure 3 showed that the water drop measured

in the Ti samples modified by Mo presented a slightly more hydrophilic behaviour than those presented in Ti-Nb surfaces, except for Ti-Nb_{NH4Cl} and Ti-Mo_{NH4Cl} which presented the value (91.3 ^{o}). It could be attributed to the TiN on surface formed by NH_4Cl addition. The most hydrophobic behaviour was found for the Ti-Nb_{coat} sample which also exhibited the highest roughness value. However, bare Ti and Ti-Nb presented similar contact angle values around 83 ^{o}. As far as surface roughness is concerned, the bare Ti material presented smaller value (0.65 μm) while mild increases were found for the surface modified samples attributed to the surface modification process. It could be stated that in order of roughness the materials with Nb showed the following: Ti-Nb (1.38 μm), Ti-Nb_{NH4Cl} (1.8 μm) and Ti-Nb_{coat} (2.2 μm). The Ti-Mo samples showed a bit more hydrophilic behaviour and the roughness values were slightly lower. Therefore, in the order to smoother surfaces the following values were obtained: Ti-Mo (0.66 μm), Ti-Mo_{coat} (0.82 μm) and Ti-Mo_{NH4Cl} (1.36 μm). Similar roughness and wettability values were reported by [15] since contact angles in the order of 80-90 ^{o} are desirable for cell attachment and proliferation, and rougher surfaces are considered more beneficial than smoother for osseointegration and bone formation [28].

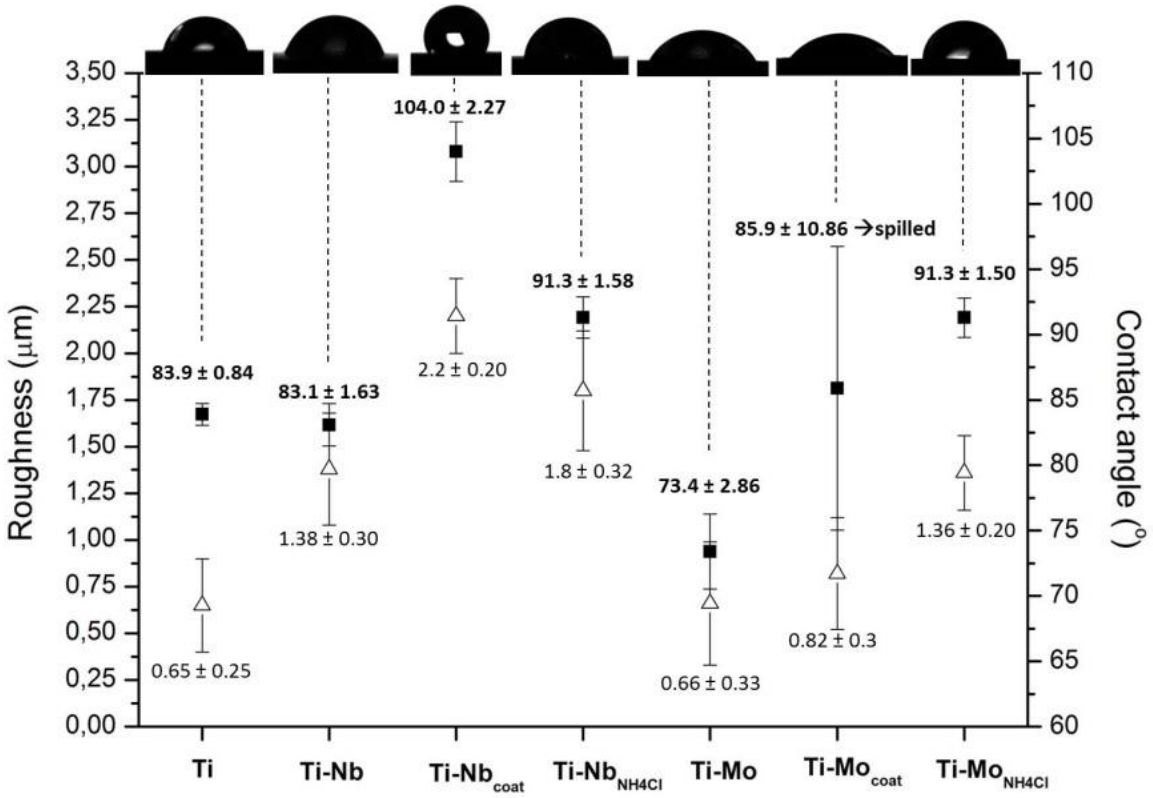

Figure 3. Surface roughness (△) and contact angle (■) values for Ti and the designed modified PM Ti materials. Roughness results expressed as triplicate and wettability results as Mean ± S.E.M. (Standard Error of Mean) from 3 samples (in total 6 measurements of each material).

3.3 *In vitro* bioactivity in SBF: apatite-forming ability

One requirement for a biomaterial to be considered suitable for bone replacement applications is to present bone bonding ability, e.g. able to generate a strong bonding to bone, such property is called bioactivity. In the present study, the potential bioactive character of the modified Ti based materials was tested through immersion in SBF, a well-known method to test the hydroxyapatite formation ability of materials, being a useful method to predict the bioactivity of materials [18].

At this stage, it is worth pointing out that since these modified Ti surfaces were designed with enhanced surface properties, e.g. improved micro-hardness and lower elastic modulus [23], the main aim of this work is to test these surfaces without modifying them. Therefore, no additional surface treatments were performed to induce hydroxyapatite formation. For this reason, the hydroxyapatite formation ability of these

different modified Ti surfaces was tested in SBF for 14 and 21 days, and it was compared to that of the unmodified Ti sample. These immersion times were selected due to metals without pre-treatment requires longer times to promote a bone-like apatite layer as [29]. Moreover, it was reported that 21 days of immersion time led to a dense and uniform apatite layer on Ti under different surface roughness conditions [30].

As summarized in Table 1, the surfaces were tested in SBF with the following surface states: Ground-1200# (Ti-Nb, Ti-Mo, Ti-Nb_{NH4Cl} and Ti-Mo_{NH4Cl}), as-coated (Ti-Nb_{coat} and Ti-Mo_{coat}) and polished- 1μm (Ti). Figure 4 shows the FTIR spectra of the tested materials after soaking in SBF for 14 and 21 days ranging from 400 to 4000 cm^{-1} (Figure 4a) together with exemplary XRD spectra (Figure 4b-c). As it can be seen in Figure 4a, both FTIR spectra showed similar peaks, although those formed for the longer immersion time of 3 weeks (right) appeared better defined than those corresponding to the immersion time of 2 weeks (left). The strongest bands, at 563, and 1061 cm^{-1}, were attributed to the PO_4^{-3} group, as well as the less intensive one at 605 cm^{-1}; confirming the formation of hydroxyapatite [16]. Moreover, the characteristic bands of the carbonate group were observed at 873 and 1423 cm^{-1}; and the band at 2300 cm^{-1} was assigned to a CO group. Finally, those formed at 1640 and 3725 cm^{-1} corresponded to water compound. These results were in good agreement with the carbonated apatite reported by [31] and [30]. Additionally, these results must be correlated with SEM and XRD information in order to compare morphology and structure. Since the peaks attributed to hydroxyapatite were well formed after 21 days of immersion, the further XRD and SEM results were focused on these samples. Therefore, the x-ray diffraction spectrum after 21 days of immersion in SBF is shown in Figure 4b. For this analysis, three materials were selected as examples (Ti, Ti-Nb and Ti-Nb_{NH4Cl}) due to the similar results revealed by FTIR and SEM. The diffraction peaks

with higher intensity attributed to apatitic Ca-P appeared at the 2θ values of 30.2° and 37.3°, while those less intensive were found at 32° and 51.9° 2θ. This is supported with apatite peaks formed from SBF immersion [30] and compared to the XRD pattern of a biomimetic apatite layer reported in a recent work [32]. The relatively broad and low intensity of the apatite peaks could suggest low degree of crystallinity or small crystal sizes. Moreover, peaks attributed to TiN, Nb or α/β-Ti can be detected, indicating that the hydroxyapatite has been partially formed. The phase composition and a detailed view of the hydroxyapatite peaks are presented in Figure 4b and c, respectively. The calcium hydroxyapatite phase showed values from 15 to 22 % for Ti-Nb and Ti-Nb_{NH4Cl}, respectively. This was obtained by Rietveld analysis of the DRX spectra taking into account the whole diffractogram in order to avoid surface texture. The presence of hydroxyapatite pointed out the bioactive character of these surfaces.

a)

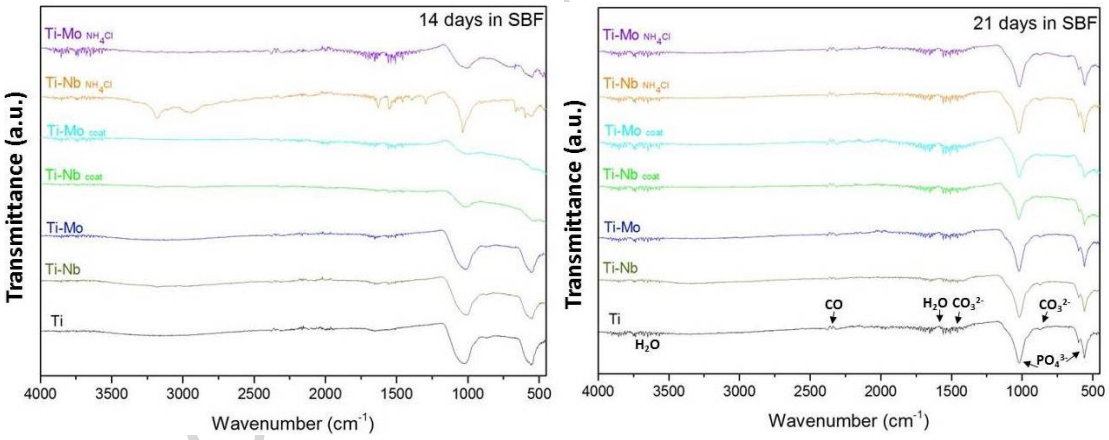

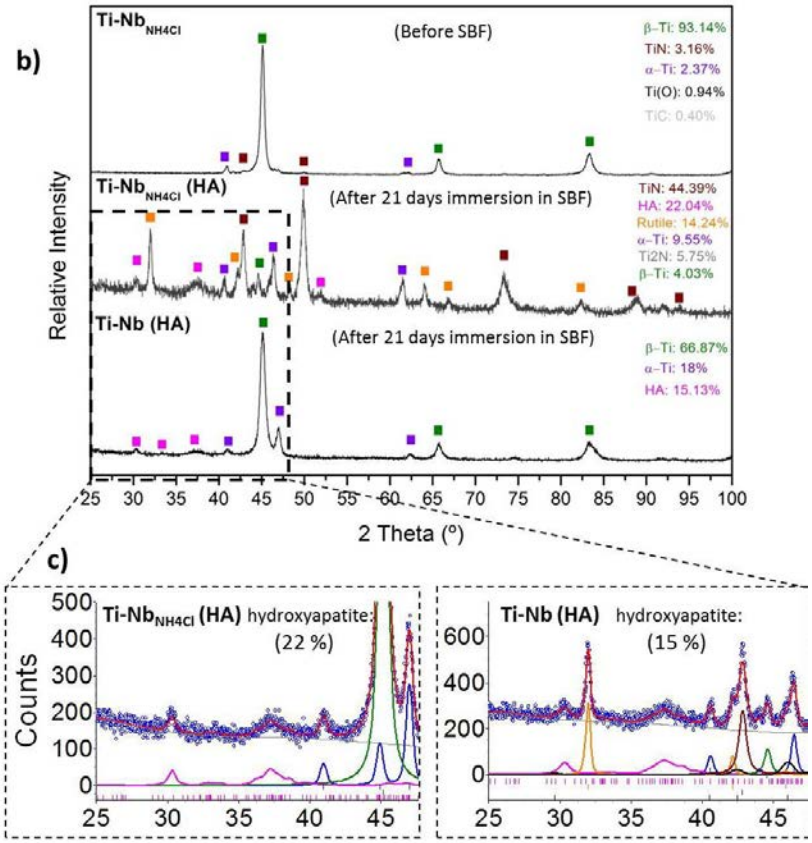

Figure 4. a) FTIR spectra for the surfaces after immersion in SBF for: 14 days (left) and 21 days (right). b) XRD spectra showing the phases composition of two selected samples: Ti-Nb$_{NH4Cl}$ and Ti-Nb, after immersion in SBF for 21 days; and c) detailed view of the XRD pattern after Rietveld fitting showing hydroxyapatite grown on Ti-Nb$_{NH4Cl}$ and Ti-Nb.

Generally, it has been speculated that titanium could not exhibit apatite formation unless it was induced by surface treatments such as an alkali-treatment. This has been the most employed method consisting of soaking in NaOH plus a subsequent heat treatment. This led to the formation of Ti-OH groups on surface and thus, treated metals could present apatite formation [18]. This treatment is usually found in literature to promote the apatite formation on Ti alloys; however there is evidence that Ti alloys after mechanical treatment such as grinding and sand-blasting present hydroxyapatite formation [5]. Moreover, for Ti alloys, it has been reported that on long term apatite formation depends on the alloy composition, and Nb addition is found to be helpful for the nucleation and growth of calcium phosphates [20], [11]. Figure 5 shows the precipitates on the surfaces of all the modified materials and Ti control after 21 days of immersion

in SBF. The precipitates appeared homogenously distributed over the surface; forming a hydroxyapatite layer. The layer was formed similarly in all the surfaces, showing a dense and well-defined cauliflower structure. Similar results were also reported by [5], and analogous structures of apatite layer formed on NaOH-heat treated Ti metal after 4 weeks have been reported by [18], [33]. Figure 5b (Ti-Mo) presented some cracks in the HA layer usually formed due to the drying process in ambient air. This led to a pore with the inner part covered by hydroxyapatite which allows observing the dense HA layer. Moreover, in Ti-Nb_{NH4Cl}, Ti-Mo_{coat} and Ti-Mo_{NH4Cl} some overlapping outcrops of hydroxyapatite were formed above the homogeneous HA layer. It points out the bioactive character of the modified Ti surfaces by Nb and Mo, showing apatite-inducing ability in SBF.

These results are in agreement with the recent work [34] where the mechanism of apatite formation on Nb-Ti-Ta was interpreted as electrostatic interactions between the ions of SBF and the surface. Therefore, it can be deduced that the Nb-OH and Ti-OH groups formed on the surfaces together with the porosity were positive for increasing the active sites for the hydroxyapatite growth and nucleation.

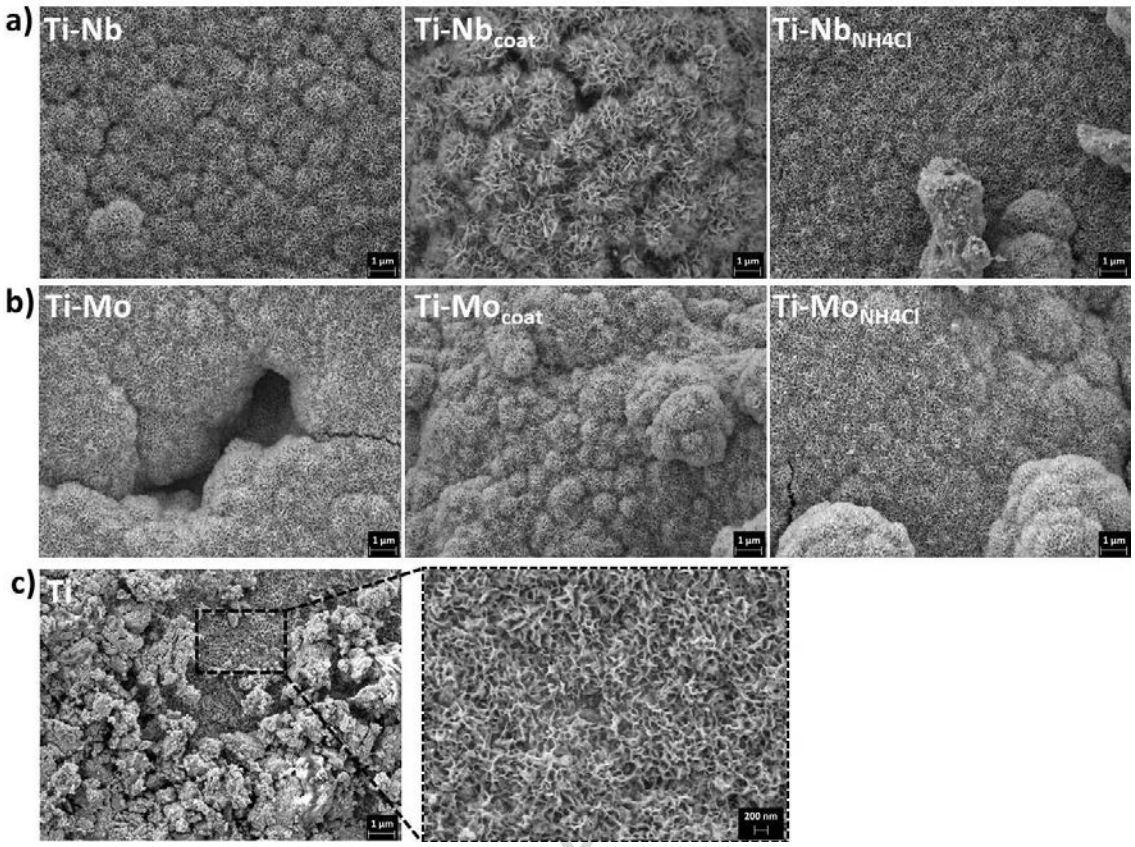

Figure 5. FE-SEM micrographs obtained from: a) the three different designed Ti-Nb surfaces, b) the three different designed Ti-Mo surfaces, and c) the Ti control surface; after 3 weeks immersion in SBF. They show the hydroxyapatite with cauliflower structure.

The EDS image mapping of the surfaces after immersion in SBF for 21 days is presented in Figure 6. The presence and distribution of both Ca and P was confirmed, verifying the hydroxyapatite detected in SEM images in Figure 5. The mappings performed on Ti-Nb and Ti-Nb$_{coat}$ presented a very homogeneous aspect and they were compared to Ti surface. The Ca and P distribution as well as the Ca/P ratio for the three surfaces were shown in order to compare it to the hydroxyapatite stoichiometric molar ratio (1.67). As far as the Ca and P distribution is concerned, the three surfaces offered homogeneous and uniformed distribution. Nevertheless, the different morphologies observed could be attributed to the difference in surface roughness since Figure 6a corresponds to a rougher surface (Ti-Nb$_{coat}$) and Figure 6b-c, to a smoother Ti-Nb and Ti surface, respectively. The mappings showed similarity to those of Ca, P and Nb

reported by [16]. Regarding the Ca/P ratio, Ti-Nb and Ti obtained lower values (≈ 1.05) while the value for the Ti-Nb_{coat} was of 1.9, closer to the stoichiometric one (1.67).

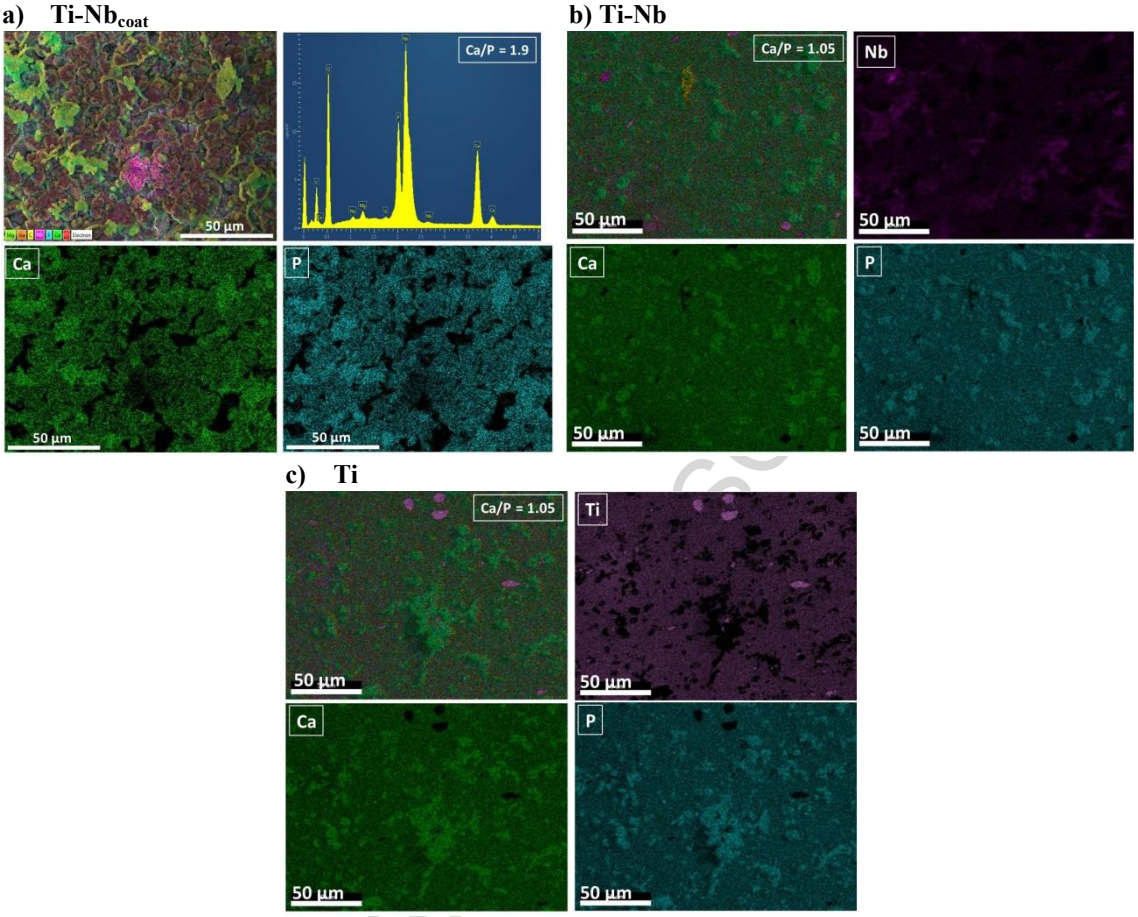

Figure 6. EDS image mapping showing the Ca and P distribution of the hydroxyapatite layer formed on: a) Ti-Nb_{coat}, b) Ti-Nb and c) Ti after 21 days immersion in SBF

3.4 Biological response

The cellular behaviour of MG-63 cells was studied in the Ti-Nb materials, evaluating cell viability, adhesion, distribution and morphology [35]. Figure 7 shows the Calcein staining of MG-63 osteoblast-like cells in direct contact with the different material surfaces after 48 h of incubation. Living cells are identified by a green fluorescence staining; confirming good cell-material interaction represented by the great concentration of cells on all the surfaces. The cells were well adhered and spread in contact with all the surfaces. Cells on the Ti surface presented an elongated shape

(Figure 7a) while on the modified Ti surfaces, they adopted a stellate polygonal morphology with multidirectional spreading and higher connections between each other (Figure 7b-d). Images show the good cell-material interaction of all the surfaces, but especially Ti-Nb_{coat} (Figure 7c) was the most colonized with cells covering most of the surface. Therefore, the positive influence of Nb on the cell biology response is demonstrated, agreeing to other previous works based on Nb films or Nb biocermet [36], [37]. These three Ti-Nb surfaces designed with different surface conditions exhibited good cell behaviour. It could be seen that the combination of a rough (2.2 μm) and Nb-rich surface (Ti-Nb_{coat}) led to the most cell colonized surface. Moreover, the presence of a porous nitride titanium-niobium surface (Ti-Nb_{NH4Cl}) with a surface roughness value of 1.8 μm also showed positive cell-interaction. There is still a not well defined consensus about wettability in biocompatibility, since some authors report a surface hydrophilic behaviour as beneficial whereas another researches establish the hydrophobicity as more suitable for protein absorption [14]. However in these surfaces, it seems that contact angles of 90 ^{o} and 104 ^{o} are suitable for the biological response.

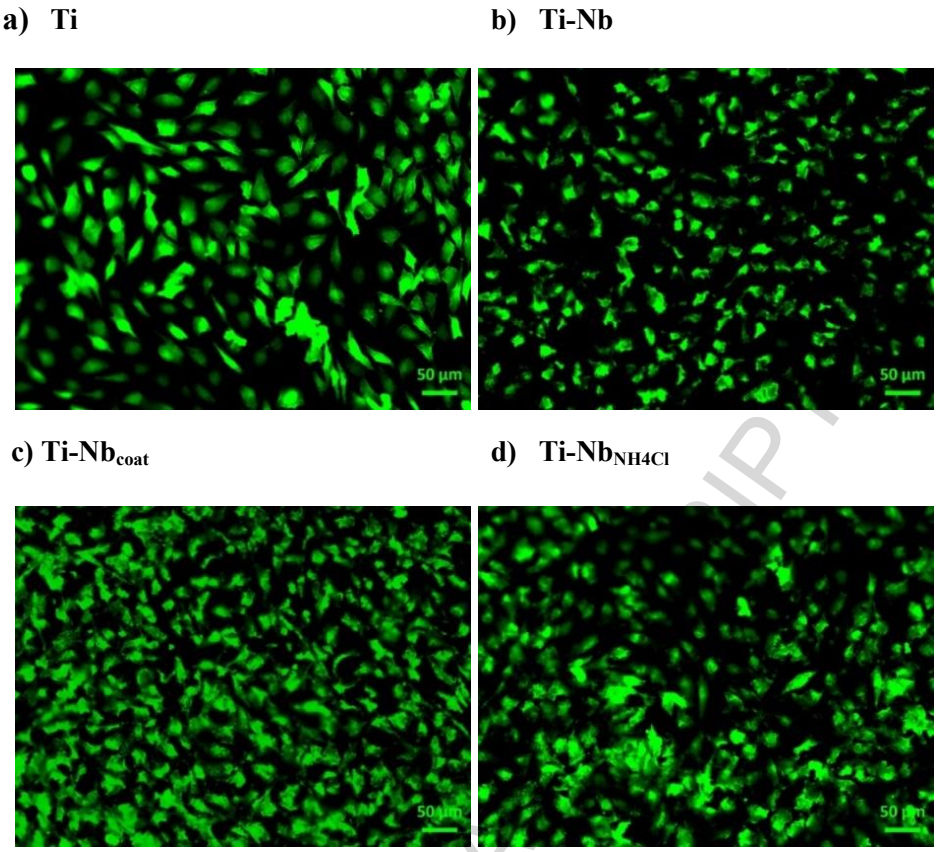

Figure 7. Live staining of MG-63 human osteoblast-like cells on: a) unmodified Ti control, b) Ti-Nb, c) Ti-Nb_{coat} and d) Ti-Nb_{NH4Cl} after 48 hours of incubation.

The cell viability of MG-63 cells assessed by WST-8 test is shown in Figure 8a. The reduction reaction of the WST-8 by dehydrogenases from cells was terminated after 90 min. This led to the yellow-orange color; pointing out the formation of formazan compound (directly proportional to the number of living cells). Therefore, the absorbance was measured at 450 nm, and the cell viability for each material was expressed as the 100 % of cell viability for the Ti sample. It can be observed the cell viability higher than 40 % (Ti-Nb), increasing for the sample Ti-Nb_{NH4Cl} (70 %) and reaching a value of 120 % for the Ti-Nb_{coat} composition. Statistically significant differences were found in relation to cell viability for Ti-Nb and Ti-Nb_{NH4Cl} compared to Ti although no significant differences (p<0.05) were detected between Ti-Nb_{coat} and Ti. These results were compared not only to the qualitative information from the CLSM images (Figure 7), but also to quantitative information obtained from ImageJ analysis

(Figure 8b) where the number of cells adhered to the different surfaces is presented. The result for each surface is showed as the average of an overview image of a 500 μm area of two different samples. The cell number for the Ti-Nb was similar to the Ti while a higher concentration of adhered cells was detected for Ti-Nb_{NH4Cl} and Ti-Nb_{coat} samples (around 7500 and 12000), respectively. This shows good agreement with the cell viability where both of them exhibited the highest proliferation, as well as with the fluorescence images (Figure 7c-d). According to these results, it can be confirmed that the Nb diffusion has not induced any cytotoxic effect.

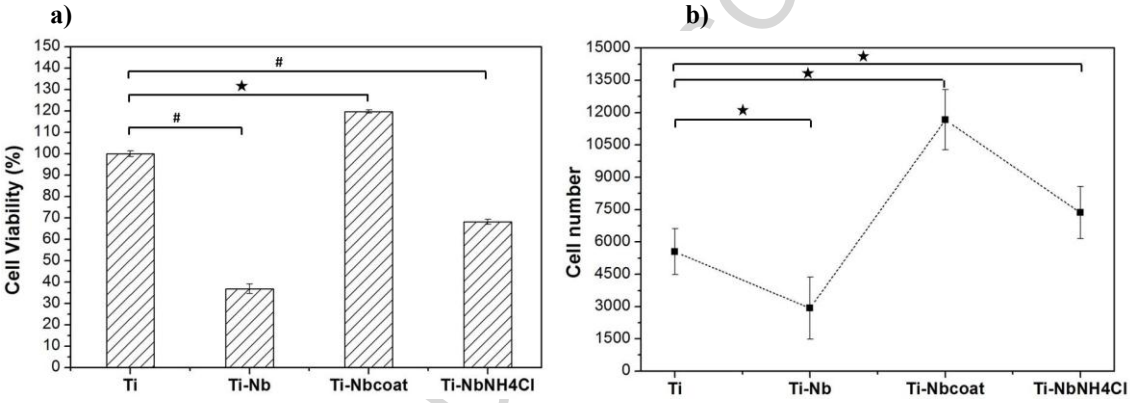

Figure 8. a) Cell viability and b) number of cell adhered to the surfaces (by ImageJ analysis) of MG-63 cells cultured on: unmodified Ti, Ti-Nb, Ti-Nb_{coat} and Ti-Nb_{NH4Cl} after 48 hours of incubation. Cell viability results expressed as mean ± standard deviation of 5 samples (in total 10 measurements of each material). Cell number expressed as mean ± standard deviation of 3 samples (in total 6 measurements of each material). ★ *$p<0.05$ is statistically insignificant and # $p>0.05$ statistically significant compared to Ti.*

Further examination of the morphology adopted by the human osteoblast-like cells on the surfaces was performed by SEM. The overview and detailed observation of the MG-63 cells grown on the different surfaces after 2 days of incubation is shown in Figure 9. The general view of all the samples shows a high number of cells covering the whole surfaces in all the samples as indication of the cell adhesion. Furthermore, the micrographs at higher magnification proved the well spread of the cells and the connection and linking between each other promoting the cell-cell communication. All the surfaces established connection with the neighboring cells; nevertheless the three

modified Ti surfaces seemed to enhance their cell activity due to the existence of a major number of cell-cell communication and better surface interaction. It would be worth it to notice that cells could anchor on these surfaces as well as into the internal pores due to the porosity created in them (Figure 9b-d). Therefore, it was demonstrated that the surface modification by niobium diffusion treatments led to different Ti-Nb designed with determined surface roughness and wettability conditions with suitable cell-material interaction.

a) Ti

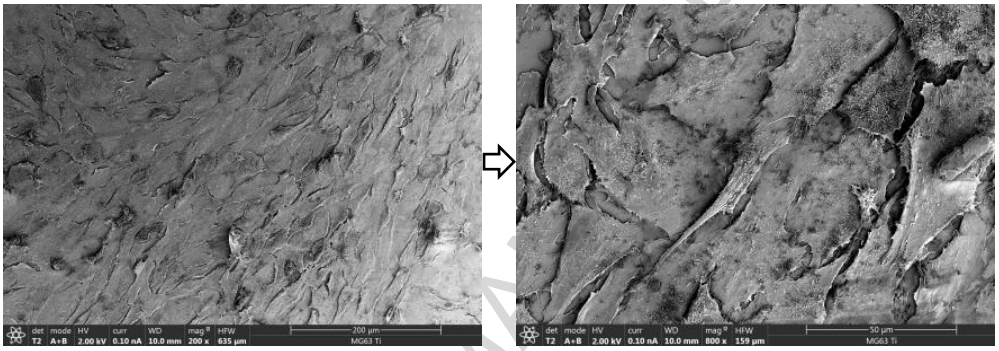

b) Ti-Nb

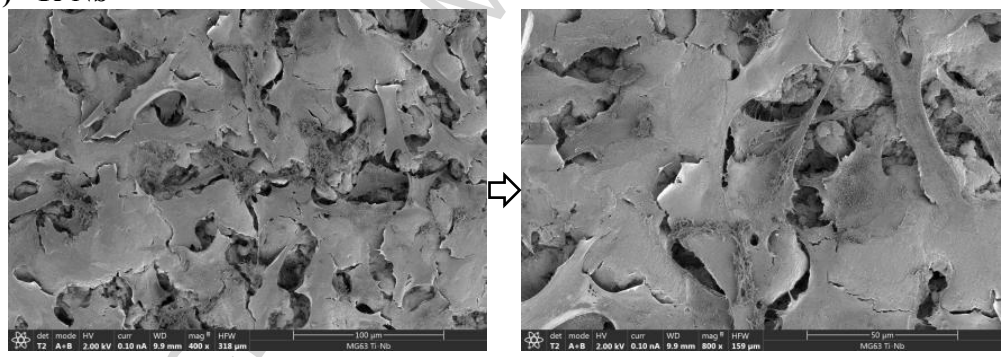

c) Ti-Nb$_{coat}$

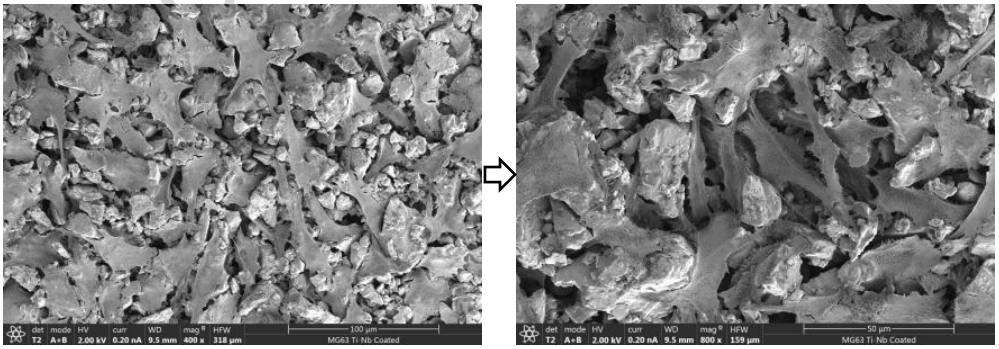

d) Ti-Nb$_{NH4Cl}$

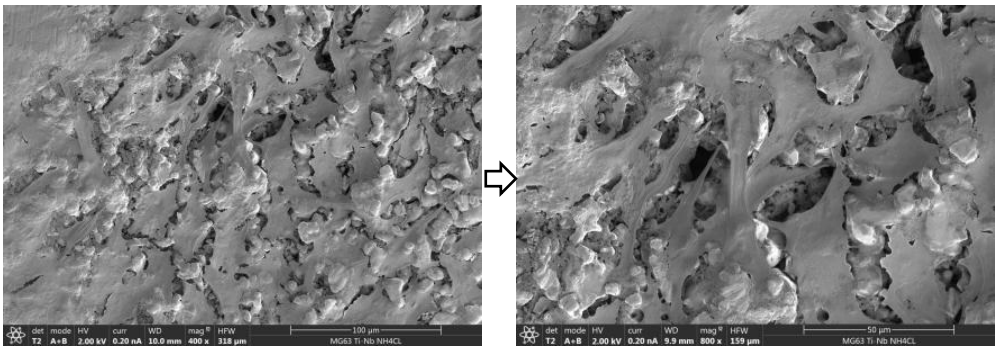

Figure 9. FE-SEM images from low (left) to high (right) magnification of MG-63 human osteoblast-like cells cultured on a) unmodified Ti control, b) Ti-Nb, c) Ti-Nb_{coat} and d) Ti-Nb_{NH4Cl} after 48 hours of incubation.

4. Conclusions

This work relied on the first approach of the bioactivity and cellular behaviour of a new family of modified Ti surfaces (Ti-Nb, Ti-Nb_{coat}, Ti-$Nb_{NH4Cl,}$ Ti-Mo, Ti-Mo_{coat}, Ti-Mo_{NH4Cl}) designed with β-phase surface and enhanced mechanical performance.

In this study, the reactivity of all the modified Ti surfaces (Ti-Mo and Ti-Nb) was tested by immersion in SBF during 14 and 21 days; leading to positive results in terms of bioactivity due to their ability of hydroxyapatite formation. The results were presented and compared considering the surface physico-chemical properties: i) composition (Ti-Nb/Mo), ii) roughness (Ti-Nb/Mo_{coat}), and iii) porosity (Ti-Nb/Mo_{NH4Cl}). Additionally, it was demonstrated that the surfaces exhibited suitable roughness and wettability conditions to promote a bone-like apatite layer after 21 days of immersion in SBF, without any additional pre-treatment to promote it.

Regarding the *in vitro* cellular behaviour of osteoblast-like cells (MG-63) on Ti-Nb surfaces, positive cell viability and cell-material interaction was obtained for all the surfaces. However, the highest cell viability was presented by the surface designed with 99 % of Nb, 2.2 µm of roughness and a 104 ^{O} contact angle (Ti-Nb_{coat} surface).

Therefore, it was demonstrated that the design of modified Ti surfaces through Mo and Nb diffusion treatments allowed obtaining bioactive surfaces with positive cell-material

interaction. Further results related to the osteogenic differentiation of bone marrow stromal cells on these β-Ti surfaces will be provided in a forthcoming article in order to fully evaluate their potential for bone replacement application.

Acknowledgment

The authors would like to thank the funding provided for this research by the Regional Government of Madrid (program MULTIMAT-CHALLENGE-CM, ref. S2013/MIT-2862), and by the University Carlos III of Madrid for the research stay of three months in the Institute of Biomaterials (University of Erlangen-Nurnberg).

References

[1] L. Kunčická, R. Kocich, and T. C. Lowe, "Advances in Metals and Alloys for Joint Replacement," *Prog. Mater. Sci.*, no. April, 2017.

[2] M. Geetha, a. K. Singh, R. Asokamani, and a. K. Gogia, "Ti based biomaterials, the ultimate choice for orthopaedic implants - A review," *Prog. Mater. Sci.*, vol. 54, no. 3, pp. 397–425, 2009.

[3] X. Yang and C. R. Hutchinson, "Corrosion-wear of beta-Ti alloy TMZF (Ti-12Mo-6Zr-2Fe) in simulated body fluid," *Acta Biomater.*, vol. 42, pp. 429–439, 2016.

[4] M. Niinomi, "Mechanical biocompatibilities of titanium alloys for biomedical applications," *J. Mech. Behav. Biomed. Mater.*, vol. 1, no. 1, pp. 30–42, 2008.

[5] P. F. Gostin, A. Helth, A. Voss, R. Sueptitz, M. Calin, and A. Gebert, "Surface treatment, corrosion behavior, and apatite-forming ability of Ti-45Nb implant alloy," *J. Biomed. Mater. Res. B Appl. Biomater.*, vol. 101B, no. 2, pp. 269–278, 2013.

[6] P. Neacsu, D. Gordin, V. Mitran, T. Gloriant, M. Costache, and A. Cimpean, "In vitro performance assessment of new beta Ti–Mo–Nb alloy compositions," *Mater. Sci. Eng. C*, vol. 47, pp. 105–113, 2015.

[7] V. S. A. Challa and R. D. K. Misra, "Reduced toxicity and superior cellular response of preosteoblasts to Ti-6Al-7Nb alloy and comparison with Ti-6Al-4V," *J. Biomed. Mater. Res. A*, vol. 101A, no. 7, pp. 2083–2089, 2013.

[8] B. Michael, J. Christian, J. Schantz, U. Gbureck, L. Rackwitz, U. Nöth, F. Jakob, M. Rudert, J. Groll, and D. Werner, "How smart do biomaterials need to be ? A translational science and clinical poin t of view," *Adv. Drug Deliv. Rev.*, vol. 65, no. 4, pp. 581–603, 2013.

[9] A. Kazek-ke, K. Kuna, W. Dec, M. Widziołek, G. Tylko, A. M. Osyczka, and W. Simka, "In vitro bioactivity investigations of Ti-15Mo alloy after electrochemical surface modification," *J. Biomed. Mater. Res. B Appl. Biomater.*, vol. 104B, no. 5, pp. 903–913, 2016.

[10] T. Kokubo, H. Kim, and M. Kawashita, "Novel bioactive materials with different mechanical properties," *Biomaterials*, vol. 24, pp. 2161–2175, 2003.

[11] K. C. Nune, R. D. K. Misra, S. J. Li, Y. L. Hao, and R. Yang, "Osteoblast cellular activity on low elastic modulus Ti-24Nb-4Zr-8Sn alloy," *Dent. Mater.*, vol. 33, pp. 152–165, 2017.

[12] V. Goriainov, R. Cook, J. M. Latham, D. G. Dunlop, and R. O. C. Oreffo, "Bone and metal: An orthopaedic perspective on osseointegration of metals," *Acta Biomater.*, vol. 10, no. 10, pp. 4043–4057, 2014.

[13] P. Mandracci, F. Mussano, P. Rivolo, and S. Carossa, "Surface Treatments and Functional Coatings for Biocompatibility Improvement and Bacterial Adhesion Reduction in Dental Implantology," *Coatings*, vol. 6, no. 7, pp. 1–22, 2016.

[14] M. Z. Ibrahim, A. A. D. Sarhan, F. Yusuf, and M. Hamdi, "Biomedical materials and techniques to improve the tribological , mechanical and biomedical properties of orthopedic implants - A review article," *J. Alloys Compd.*, vol. 714, pp. 636–667, 2017.

[15] Y. Bai, Y. Deng, Y. Zheng, Y. Li, R. Zhang, Y. Lv, Q. Zhao, and S. Wei, "Characterization, corrosion behavior, cellular response and in vivo bone tissue compatibility of titanium–niobium alloy with low Young â€™s modulus," *Mater. Sci. Eng. C*, vol. 59, pp. 565–576, 2016.

[16] V. S. Ciminelli and H. S. Mansur, "Niobium-Doped Hydroxyapatite Bioceramics: Synthesis, Characterization and In Vitro Cytocompatibility," *Materials (Basel).*, vol. 8, pp. 4191–4209, 2015.

[17] R. Olivares-navarrete, J. J. Olaya, and C. Ramírez, "Biocompatibility of Niobium Coatings," *Coatings*, vol. 1, pp. 72–87, 2011.

[18] T. Kokubo and H. Takadama, "How useful is SBF in predicting in vivo bone bioactivity?," *Biomaterials*, vol. 27, pp. 2907–2915, 2006.

[19] M. W. D. Mendes, C. G. Ágreda, A. H. A. Bressiani, and J. C. Bressiani, "A new titanium based alloy Ti–27Nb–13Zr produced by powder metallurgy with biomimetic coating for use as a biomaterial," *Mater. Sci. Eng. C*, vol. 63, pp. 671–677, 2016.

[20] J. Mystkowska, P. Deptula, J. Kolmas, and J. R. Dabrowski, "Surface activity of titanium alloys contacted with the simulated body fluid," *J. Vibroengineering*, vol. 11, no. 4, pp. 725–728, 2009.

[21] D. Perez, D. Andrade, L. Marotta, R. De Vasconcellos, I. Chaves, S. Carvalho, L. Ferraz, D. B. Penna, E. Luzia, D. S. Santos, R. Falchete, D. Roberto, C. Alberto, A. Cairo, and Y. Rodarte, "Titanium–35niobium alloy as a potential material for biomedical implants: In vitro study," *Mater. Sci. Eng. C*, vol. 56, pp. 538–544, 2015.

[22] I. Jirka, M. Vandrovcová, O. Frank, J. Pl, T. Luxbacher, L. Ba, and V. Starý, "On the role of Nb-related sites of an oxidized β-TiNb alloy surface in its interaction with osteoblast-like MG-63 cells," *Mater. Sci. Eng. C*, vol. 33, pp. 1636–1645, 2013.

[23] J. Ureña, E. Tejado, J. Y. Pastor, F. Velasco, S. Tsipas, A. Jiménez-Morales, and E. Gordo, "Role of beta-stabilizer elements in microstructure and mechanical properties evolution of PM modified Ti surfaces designed for biomedical applications," *Euro PM 2017 Proceedings, ISBN 978-1-899072-49-1*, 2017.

[24] B. Sharma, S. Kumar, and K. Ameyama, "Microstructure and properties of beta Ti-Nb alloy prepared by powder metallurgy route using titanium hydride powder," *J. Alloys Compd.*, vol. 656, pp. 978–986, 2016.

[25] J. Ureña, C. Mendoza, B. Ferrari, Y. Castro, S. A. Tsipas, A. Jiménez-Morales, and E. Gordo, "Surface Modification of Powder Metallurgy Titanium by Colloidal Techniques and Diffusion Processes for Biomedical Applications," *Adv. Eng. Mater.*, vol. DOI: 10.10, pp. 1–8, 2016.

[26] S. A. Tsipas and E. Gordo, "Molybdeno-Aluminizing of Powder Metallurgy and Wrought Ti and Ti-6Al-4V alloys by Pack Cementation process," *Mater. Charact.*, vol. 118, pp. 494–504, 2016.

[27] J. T. Ninomiya, J. A. Struve, J. Krolikowski, M. Hawkins, and D. Weihrauch, "Porous ongrowth surfaces alter osteoblast maturation and mineralization," *J. Biomed. Mater. Res. A*, vol. 103A, no. 1, pp. 276–281, 2015.

[28] X. Dai, X. Zhang, M. Xu, Y. Huang, and C. Heng, "Synergistic effects of elastic modulus and surface topology of Ti-based implants on early osseointegration," *RSC Adv.*, vol. 6, pp. 43685–43696, 2016.

[29] T. Kokubo, "Apatite formation on surfaces of ceramics, metals and polymers in body environment," *Acta mater*, vol. 46, no. 7, pp. 2519–2527, 1998.

[30] X. Chen, Y. Li, P. D. Hodgson, and C. Wen, "Microstructures and bond strengths of the calcium phosphate coatings formed on titanium from different simulated body fl uids," *Mater. Sci. Eng. C*, vol. 29, no. 1, pp. 165–171, 2009.

[31] A. L. B. Mac, B. K. Esther, M. V. Kathryn, R. K. Brow, D. E. Day, A. Hoppe, A. R. Boccaccini, M. Vallet-regı, A. V Teixeira, Y. Vueva, R. M. Almeida, M. Miola, J. R. Jones, and C. V. E. Verne, "A unified in vitro evaluation for apatite-forming ability of bioactive glasses and their variants," *J Mater Sci Mater Med*, vol. 26, no. 115, pp. 1–10, 2015.

[32] L. Liu, J. Xu, and S. Jiang, "Nanocrystalline β-Ta Coating Enhances the Longevity and Bioactivity of Medical Titanium Alloys," *Metals (Basel).*, vol. 6, no. 221, pp. 1–27, 2016.

[33] X. Liu, P. K. Chu, and C. Ding, "Surface modification of titanium, titanium alloys, and related materials for biomedical applications," *Mater. Sci. Eng. R Reports*, vol. 47, no. 3–4, pp. 49–121, 2004.

[34] J. Liu, L. Chang, H. Liu, Y. Li, H. Yang, and J. Ruan, "Microstructure, mechanical behavior and biocompatibility of powder metallurgy Nb-Ti-Ta alloys as biomedical material," *Mater. Sci. Eng. C*, vol. 71, pp. 512–519, 2017.

[35] A. Hoppe, J. Will, R. Detsch, A. R. Boccaccini, and P. Greil, "Formation and in vitro biocompatibility of biomimetic hydroxyapatite coatings on chemically treated carbon substrates," *J. Biomed. Mater. Res. A*, vol. 102A, no. 1, pp. 193–203, 2014.

[36] J. S. Moya, R. Couceiro, C. F. Guti, and A. Martinez-Insua, "In vitro and in vivo evaluation of a new zirconia/niobium biocermet for hard tissue replacement," *Biomaterials*, vol. 76, pp. 313–320, 2016.

[37] G. Ramírez, S. E. Rodil, H. Arzate, S. Muhl, and J. J. Olaya, "Niobium based coatings for dental implants," *Appl. Surf. Sci.*, vol. 257, pp. 2555–2559, 2011.

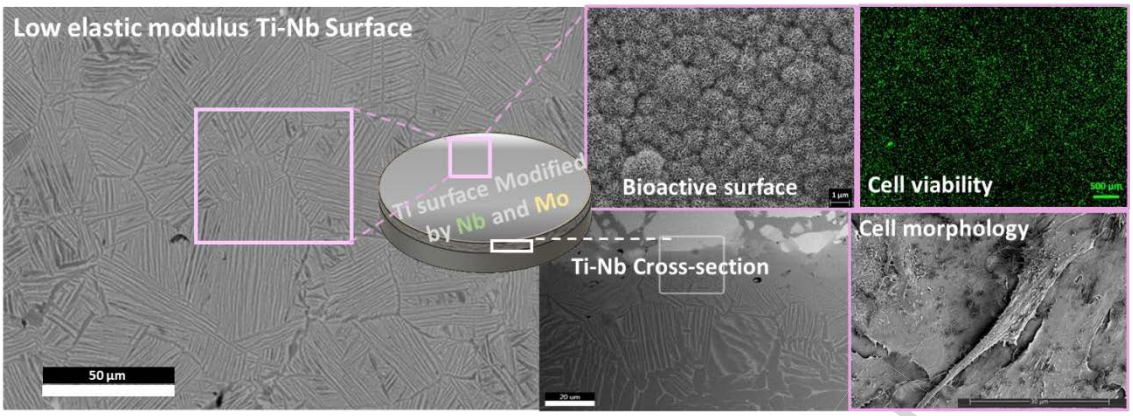

Graphical abstract

Highlights

- The surface modification of Ti by Mo or Nb diffusion processes decrease elastic modulus and enhance bioactivity.
- Ti surfaces modified with Mo and Nb show ability for hydroxyapatite formation without additional pre-treatments to promote it.
- Improved cell-material interaction of the different Ti-Nb surfaces designed compared to Ti.